

Online MEMS-Based Specific Gravity Measurement for Lead-Acid Batteries

Yashwant Gulab Adhav^{1,*}, Dayaram Nimba Sonawane², Chetankumar Yashawant Patil²

¹Department of Instrumentation and Control Engineering, Cummins College of Engineering for Women, Pune, India

²Department of Instrumentation and Control Engineering, College of Engineering, Pune, India

Received 24 November 2021; received in revised form 23 January 2022; accepted 30 January 2022

DOI: <https://doi.org/10.46604/aiti.2022.8964>

Abstract

Traditional methods for measuring the specific gravity (SG) of lead-acid batteries are offline, time-consuming, unsafe, and complicated. This study proposes an online method for the SG measurement to estimate the state-of-charge (SoC) of lead-acid batteries. This proposed method is based on an air purge system integrating with a micro electro mechanical system sensor. The system's performance is compared against the glass hydrometer, a reference standard, to evaluate its effectiveness. Through the proposed strategy, the SoC measurement achieves up to $\pm 1\%$ accuracy. The technique has an SG accuracy of $\pm 0.002\%$ which is better than the glass hydrometer accuracy of $\pm 0.005\%$ in the battery charge reading. The experimental results show that the high accuracy and precise measurements of SG and SoC can be conducted by using the proposed method.

Keywords: Kordash chart, lead-acid batteries, MEMS, specific gravity, temperature compensation

1. Introduction

Most energy storage systems require batteries to function [1-3]. Currently, lead-acid batteries, lithium-ion batteries, and fuel cells are employed as power backup sources. Lead-acid batteries are used in various power-generation fields, such as solar power systems, wind power plants, uninterrupted power systems, automotive vehicles, smart grid systems, and aircraft [4-6].

Since the last century, lead-acid batteries have been on the market due to their low cost, recyclable material, high power density, and consistent output regardless of the environment. No commercial online sensor is available in the market that can gauge the state-of-charge (SoC) of a lead-acid battery using a measurement of specific gravity (SG). Larger lead-acid batteries are utilized in underwater vehicles, such as submarines, to start the engines as they require a larger amount of current. SoC estimation based on SG is more accurate than the voltage and current method, but measuring the SG of acid is a challenging and tough task.

To measure the SG using conventional methods, a sensor has to overcome several vital constraints inside the battery. It is important to resist acid corrosion as the sensor comes in contact with the acid. During the charging and discharging processes, the sensor has to compensate for the temperature variations inside the battery because of chemical reactions. Very little space and a small quantity of acid are available at the top of the battery [7]. The constraints mentioned above can be overcome by the proposed design. This motivates the present work on lead-acid batteries. This study aims to design a sensor

* Corresponding author. E-mail address: yashwant.adhav@cumminscollege.in

and its real-time measurement system to estimate the SG of a lead-acid battery. SG predicts battery failure before the battery suffers irreparable damage. The online SG measurement displays the status of the battery like a fuel gauge. The life of a lead-acid battery is dependent on both the charging and the discharging states [8].

The novelty and leading features of the proposed work are already patented [9] and summarized as follows: (1) There has been no literature on short air purge sensing tubes that could be placed in the small space at the top of the battery. (2) After conducting the literature survey, it is observed that no researchers have proposed a micro electro mechanical system (MEMS) sensor to measure the SoC of acid batteries. (3) SoC and SG are monitored using a single sensor. (4) The change in the acid level does not affect the accuracy due to a constant head method.

The study is organized as follows: Section 2 presents the important work of sensors and techniques used to determine SoC and SG. Section 3 focuses on the pressure principle and the design of a real-time SG measurement system for the lead-acid battery. Section 4 deals with the experimental results as well as the data analysis. Section 5 presents the conclusions and future research directions.

2. Literature Review

In light of the literature review, the prevailing technique of the evaluation of SG was established by Archimedes' law. Nowadays, a hydrometer is used to measure the SoC of a lead-acid battery cell. This is a time-consuming process and cannot be performed in real-time [10]. Hence, a real-time measurement system is crucial for battery management. Non-contact methods can be utilized for online estimation, but these methods have their limitations, as mentioned below. The discharge test method is a time-consuming online method, and it modifies the state of the battery. The Ah-balancing method needs a model-based approach for error identification, and it needs periodic recalibration. The linear model approach requires reference data for fitting parameters. An artificial neural network requires training data of similar batteries. Impedance spectroscopy is temperature sensitive method and is costlier.

The DC internal resistance method is only effective for small SoCs. In the Kalman filter technique, a large computing capacity is necessary. Also, a suitable battery model is also needed, and this method has problems estimating the initial parameters [11]. A measurement of the voltage of the battery is not an accurate SoC indication because of the effects of the charge and discharge currents and the temperature variations. Before starting the open-circuit voltage measurement, the battery's current must be kept in an off state for at least 4 hours to reach an equilibrium condition [12].

Contact-type methods are best suited for online SoC measurements over non-contact methods because of the accuracy of their results. Hancke [13] developed the fiber-optic SG sensor to determine the SoC of a lead-acid battery. They applied the refractive index principle, and the method is based on the optical power loss that fibers exhibit when bent beyond a critical radius. In this technique, errors arise because of changes in the intensity of the light source and losses occur because of variations in fibers and connectors. These losses can affect the sensitivity of the sensor. Paz et al. [8] developed a polymer fiber sensor for measuring the real-time density of the electrolyte at three different locations in lead-acid batteries. The circuit was optimized with led thermal behavior. Zhao et al. [14] worked on the light return principle of reflection. When a light wave spreads in the fiber, the characteristics of the light wave, such as oscillation amplitude, phase, polarization condition, and wavelength, can change directly or indirectly as the density changes.

Patil et al. [15] developed an optical sensor based on the refractometric principle for determining the SoC of a lead-acid battery. The concentration of the acid solution and its physical characteristics were taken into consideration. Hossain and Dwyer [16] demonstrated the buoyancy principle to measure density. The float is connected to the lower arm of the core. As the float dips in the acid, the linear variable differential transformer (LVDT) generates an output signal in proportion to the

acid density variations. This system is not cost-effective, and the mechanical assembly is complicated. Morbel et al. [17] worked on the swelling and shrinkage effect of plastic in sulfuric acid. The disadvantage of this device is that the level sensing is not to be taken into consideration.

Cao-Paz et al. [18] and Lu et al. [19] measured the viscosity of the electrolyte. Density measurements are done to estimate SoC; however, the change in acid viscosity changes SoC more significantly than the change in density. In this study, there is a proposal for using a quartz crystal microbalance oscillator sensor for monitoring density and viscosity changes in lead-acid batteries. A frequency shift is observed with a change in H₂SO₄ concentration in the battery electrolyte. The biggest drawback is that calibration must be done frequently.

Heinisch et al. [20] suggested a steel tuning fork sensor having a circular and rectangular shape, which is used to measure the precise viscosity and mass density of fluids. Wilson et al. [21] used cantilever sensors excited by piezoelectric actuators to estimate the viscosity and density parameters of the fluid. Tang and Lin [22] worked on the integration of a readily available glass hydrometer and ultrasonic sensor for monitoring the density of the lead-acid battery electrolyte. In this method, two different bulky sensors were used to measure level and density.

Even if these methods are effective, the size and cost of the sensor and system are high. Inside the lead-acid battery, almost all the space is covered by lead sheets, and a very narrow space is left above the lead sheets for acid. Therefore, it is an interesting and challenging task to place the sensor at this particular location to measure SG.

3. Design of the System

3.1. Differential pressure principle

The air purge method is based on well known Pascal's pressure law [23] which reads as:

$$\Delta P = H \times \Delta \rho \times g \quad (1)$$

where ΔP is the differential pressure (Pa), H is the distance between the two tubes (m), $\Delta \rho$ is the density of acid (Kg/m³), and g is the gravitational constant (m/s²). As the differential height H and gravitational acceleration g are constant; hence, Eq. (1) shows the proportionality between ΔP and $\Delta \rho$, i.e., $\Delta P \propto \Delta \rho$.

The change in the density of the acid is directly proportional to the change in pressure. Following that, as the battery gets charged or discharged, the density of the acid changes, which changes its SG. This change in SG is directly proportional to the change in pressure. Hence, a change in pressure is directly proportional to the SoC of the battery. The head between the two tubes is considered to be 2.0 cm. The differential pressure varies from 215 Pa to 246 Pa for an SG change from 1.1 to 1.26.

3.2. SoC detection technique

Tang and Lin [22] revealed that under normal conditions, in the lead-acid battery, SG is 1.28 if SoC is 100% and SG is 1.12 if SoC is 0%. SG is directly proportional to the discharge rate of the battery by:

$$SG = 1.28 - \frac{DR}{100} \times 0.16 \quad (2)$$

where SG is specific gravity and DR is the discharge rate of the battery. As shown in Fig. 1, under normal conditions, the SG of the acid solution is linearly proportional to the SoC of the battery electrolyte.

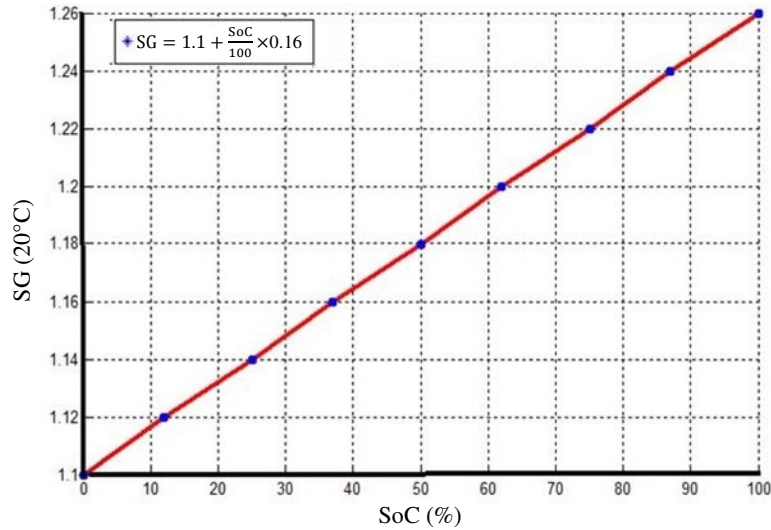


Fig. 1 SG vs. SoC

$$SG = 1.1 + \frac{SoC}{100} \times 0.16 \quad (3)$$

where SoC is the state-of-charge (%). According to the Kordash chart, SG is directly proportional to the SoC of the lead-acid battery [13]. From Eq. (3), it is concluded that the battery is 100% charged when SG is 1.26, and the battery is fully discharged when SG is 1.1.

3.3. Design of the air purge system

Fig. 2 represents a block diagram of the air purge system, which is integrated with a highly sensitive MEMS sensor. The air bubbler method is generally used for level and density measurements of a corrosive liquid [24]. The level of the fluid is monitored by measuring the back pressure using the MEMS pressure sensor to obtain high accuracy [25]. If the fluid level is kept constant, then the same method can be utilized to estimate the density of the fluid, which has been done in this study. An air purge tube is dipped through the cap of the battery in acid in such a way that it does not touch the lead sheets in the battery.

Using an aquarium mini-compressor that has a maximum pressure of 350 kPa and airflow without a load of 0.007 LPM, the air is passed through the bubbler tube. Because of hydrostatic pressure, the gas pressure in the bubbler tube continuously increases until it balances the hydrostatic pressure of the acid. When this balanced condition is reached, the back pressure in the bubbler tube remains the same as the hydrostatic pressure of the acid. As for SG, the concentration of acid increases, and the back pressure in the air purge tube increases linearly. In this case, the MPXV4006DP sensor is used to measure this back pressure. A potentiometer is used in the purge gas line to control the current of the compressor to ensure that constant bubbling action occurs at the end of the two tubes.

The unique advantage of the air purge system is that the exact location of the sensor is not very important because the pressure is the same at any location in the pipe. During charging and discharging, acid evaporates, and hence its level in the battery also decreases. This study uses the SG measurement technique using a constant head, which is independent of the change in the acid level up to a certain extent.

Acid concentration increases when the battery gets charged and decreases when the battery gets discharged. This increment or decrement in the acid concentration further increases or decreases the back pressure, which is the measure of SG. The output of the MPXV4006DP sensor is amplified using an instrumentation amplifier AD-620 [23]. Linear monolithic (LM35) sensor provides temperature compensation to reduce errors.

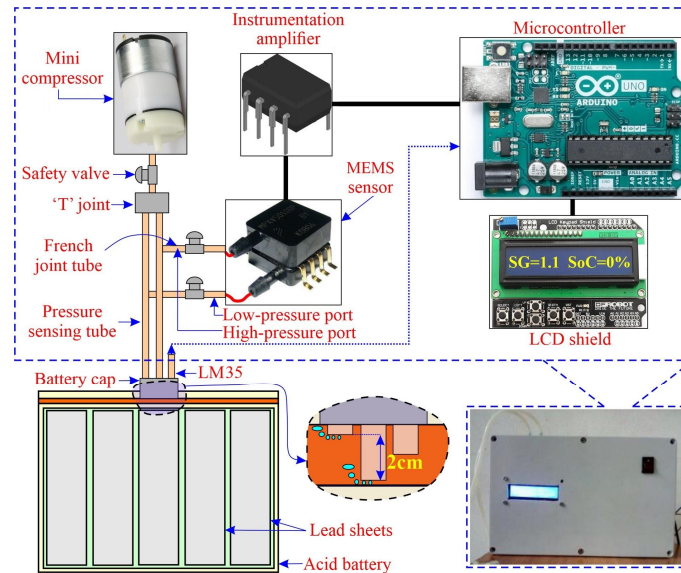


Fig. 2 SG measurement setup

The actual insertion of tubes through the battery cap is shown in Fig. 3. An air purge system is low in cost, yet it is an accurate way to measure the acid density in a battery. A complete air purge density measurement system consists of two Teflon tubes: a pressure sensor and a driving circuit for an aquarium air compressor. Mini-control valves are used to control the flow of air through the pipe.

Two separate flow-control valves are also used near the MPXV4006DP sensor port to protect the sensor from excess air pressure. The only part of the sensor that comes in contact with the acid is a Teflon dip tube, which has chemical compatibility with acid. One tube is at the upper level and the other is at the bottom level in the acid. The output of the MPXV4006DP sensor has been tested in the charged and discharged solutions. The two ends of the tubes are connected to the two ports of the MPXV4006DP sensor for monitoring differential pressure.

The most important electronic component in this system is the MPXV4006DP sensor. It has two ports: higher pressure under test is applied to the high-pressure port (marking side), while lower pressure is applied to the low-pressure port, which causes deflection of the diaphragm. Deflection and deformation are measured by calculating the change in the electrical resistance of the micro strain gauges, which are embedded in the silicon diaphragm. All four strain gauges are connected to form a Wheatstone bridge. The output of the Wheatstone bridge is directly proportional to the applied pressure [25]. These MEMS sensors have a compact size and good thermal stability because of the temperature compensation built into the sensor. The method based on the SG technique is intelligent and precise [22]. Sulfuric acid concentration measurement is the best and most reliable way of monitoring the SoC of heavy flooded-type stationary batteries [26].

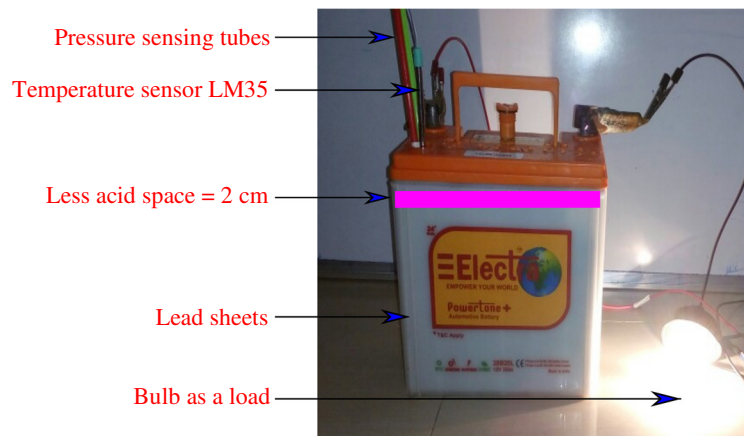


Fig. 3 Experimental setup for online SG monitoring

Table 1 shows that the output from MPXV4006DP sensor for a fully discharged battery is $v_1 = 1.355$ V. To represent this value as 0%, v_1 is tared by using a stable voltage reference of $v_2 = 1.355$ V. The output for a fully charged battery with the same sensor provides 1.661 V denoted as v_1 . It is clear that the Δv_{in} as $v_1 - v_2 = 0$ V for discharged battery and $v_1 - v_2 = 0.306$ V for a fully charged battery. To match the requirement of the microcontroller, the required signal is amplified in the range of 0 to 5 V. Hence AD-620 is used as an instrumentation amplifier with the gain calculated as $\Delta v_{in} = 0.306$ V and $v_0 = 5$ V. The gain of the amplifier is:

$$G = \frac{5V}{0.306V} = 16.33 = \frac{49.4}{R_g} + 1 \quad (4)$$

Table 1 Sensor voltage for discharge and charge battery

No.	Battery status	v_1	v_2	Δv_{in}
1	Battery discharged	1.355	1.355	0
2	Battery charged	1.661	1.355	0.306

As shown in Fig. 5, a small change in the voltage is amplified by using a gain resistor (R_g), this process is also called span compensation. This voltage range is seen to follow the straight-line linear equation used in the program to obtain a linear output from 1.100 to 1.260 SG. In the same circuit, the filtered output from the RC filter is connected to an A1 analog pin of a microcontroller consisting of a 1K resistor and a 22 μ f electrolytic capacitor used for noise reduction.

3.5. Temperature compensation using the LM35 temperature sensor

During charging and discharging, an exothermic chemical reaction takes place inside the battery. If the temperature change is low or high, this can lead to inaccurate readings. The SG of the environmental factor x_{temp} can be expressed by [22]:

$$x_{temp} = x_{20^\circ C} + [0.0007 \times (temp - 20)] \quad (5)$$

where $x_{20^\circ C}$ represents the SG of the solution at 20°C. The numbers 0.0007 and 20 are the temperature coefficients. The term $temp$ is the acid temperature of the lead-acid battery.

To determine the SG of the electrolyte under the effect of environmental parameters, the correction factor is calculated from the acid temperature is added at $x_{20^\circ C}$ temperature. This equation is valid for the temperature range of 17.8°C-54.4°C. LM35 is a more accurate and precise sensor used for temperature measurement [27]. This sensor is kept in stainless steel thermowell, and therefore, it is not subjected to the oxidation process in the battery. LM35 interfaces directly with the microcontroller without any hardware circuit. The operating temperature range of the LM35 sensor is from -55°C to 150°C. The output voltage varies by 10 mV for every 1°C variation of temperature. For the same, the SG of electrolytes at different temperatures have different SG. Temperature compensation is essential as the SG of electrolytes can change with temperature variation.

3.6. The probe construction

As shown in Fig. 6, the probe of the instrument consists of a threaded cap of the battery, which can be fitted to the battery. In this cap, two Teflon tubes of a diameter of 5 mm and the LM35 sensor are inserted through the cap of the battery. The short tube is connected to the low-pressure port, and the long tube is connected to the high-pressure port of the MPXV4006DP sensor. A small hole is provided in the cap of the battery to allow chemical gases to escape. These gases are produced because of chemical reactions during the charging and discharging of the battery.

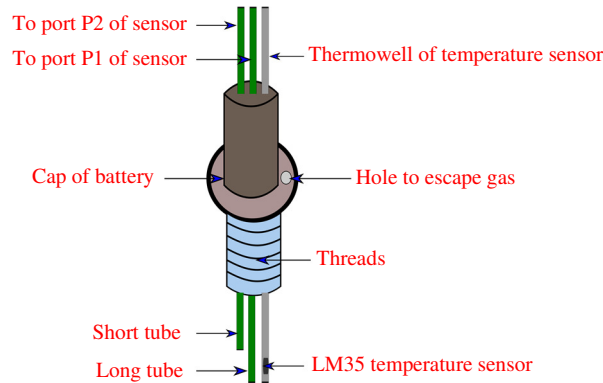


Fig. 6 Schematic of SG sensor probe

3.7. Microcontroller

An Arduino consisting of an Atmel-328, 16-MHz crystal oscillator, and 8-bit AVR is used as a microcontroller in this instrument [22]. Initially, the system is simulated using a Proteus™, and accordingly, further hardware is developed. For an analog input signal of 0 V, the microcontroller shows an SG of 1.1 and a battery charge of 1%, whereas, for the 5 V analog input signal, it displays an SG of 1.26 and a 100% battery charge. The flowchart of the proposed system is shown in Fig. 7. The SG is sensed by differential pressure sensor MPXV4006 DP. To get stability, averaging of 10 samples was done. Analog value has been read and correction of temperature, i.e., Eq. (5) compensated for accuracy. Finally, SG and battery charge (%) have been displayed on the LCD.

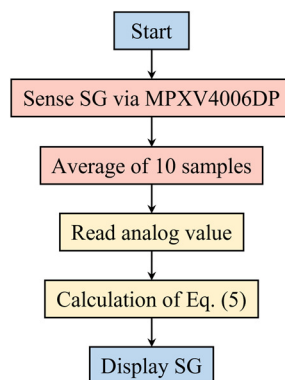


Fig. 7 Flowchart of the SG monitoring for the battery unit

3.8. Calibration

This instrument is designed in such a way that it can be calibrated and utilized for various lead-acid batteries. The procedure for calibration has been mentioned below. The probe (Teflon tube) is inserted into the discharge solution, and the zero-compensation potentiometer is adjusted to get an SG of 1.1 on the LCD shield. Later, this probe is inserted into the charged solution, and the span compensation potentiometer is adjusted to get an SG of 1.26 on display. The procedure is repeated 4-5 times for accurate calibration. The most significant advantage of the proposed system is that it can be calibrated and can be used for any kind of flooded-type lead-acid battery.

4. Results and Discussion

4.1. Repeatability and precision in the discharged condition

This section discusses the working of the present sensor for two states of the battery: one is the charge condition and the other is the discharge condition. Furthermore, to establish the effectiveness of this sensor, some parametric variations such as a change in output voltage concerning the change in SG were performed.

Two tubes of the sensor are dipped in the fully discharged acid solution. As per the reading shown by a float-type glass hydrometer, the SG of this solution is about 1.1. The tubes are withdrawn, the procedure is repeated after every 1 minute, and the experimentation is carried out on the same acid sample to check the repeatability and precision of the MEMS sensor-based hydrometer. The results are shown in Table 2 and it can be seen that the accuracy and precision of this MEMS sensor-based acidometer are highly consistent.

Table 2 Repeatability check of MEMS hydrometer (discharge acid)

No.	Amplified sensor output (V)	Battery charge (%)	SG	SG (Proteus simulation)	Battery (%) (Proteus simulation)
1	0.014	2	1.104	1.099	0
2	0.030	3	1.104	1.099	0
3	0.017	3	1.103	1.099	0
4	0.003	2	1.104	1.098	0
5	0.018	3	1.105	1.099	0

4.2. Repeatability and precision at the charged condition

Two tubes of the sensor are dipped in the fully charged acid solutions to examine the change of the instrument. As per the reading shown by a float-type glass hydrometer, the SG of this solution has been recorded as about 1.26. The above procedure is repeated to check the repeatability and precision of the MEMS sensor-based hydrometer. The results are shown in Table 3 and it can be observed that the acidometer has consistent accuracy and precision after repeated use.

Table 3 Repeatability check of MEMS hydrometer (charge acid)

No.	Amplified sensor output (V)	Battery charge (%)	SG	SG (Proteus simulation)	Battery (%) (Proteus simulation)
1	5.00	98	1.257	1.258	99
2	5.04	98	1.257	1.258	99
3	5.00	98	1.257	1.258	99
4	5.00	99	1.258	1.258	99
5	5.02	97	1.256	1.258	99

4.3. Accuracy in terms of SG

The degree of closeness to the true value is known as accuracy. The sensor has been installed on the battery. With the float-type glass hydrometer, its SG has been noted down. It is 1.192 and the voltage of the battery is 12.20 V. As shown in Fig. 8, the deviation of the measured SG is from 1.187 to 1.191. It shows that the accuracy of the system is ± 0.002 . This response has been observed for 30 minutes.

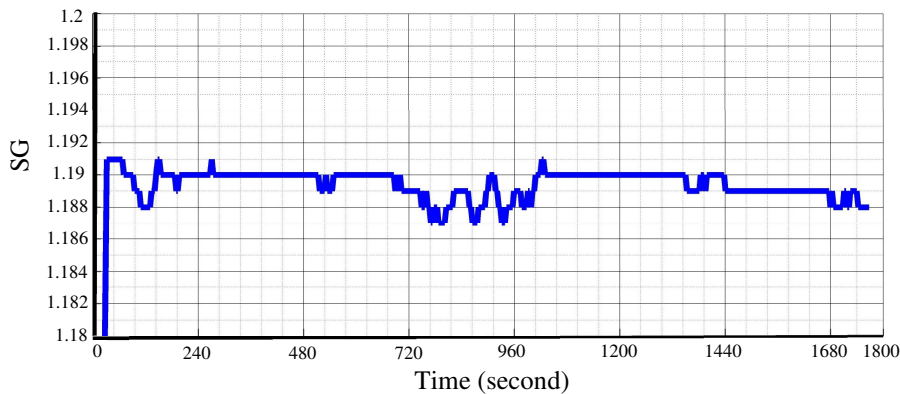


Fig. 8 SG vs. time (20°C)

4.4. Accuracy in terms of battery percentage

As shown in Fig. 9, the deviation of the measured SG is from 55% to 57%. It shows that the accuracy of the system is $\pm 1\%$ when the SG is 1.192. This response has also been observed for 30 minutes. The battery charge is measured at a true value of 56% as per the glass hydrometer reading; the proposed MEMS hydrometer indicates this value with a variation in reading of $\pm 1\%$ of the true value.

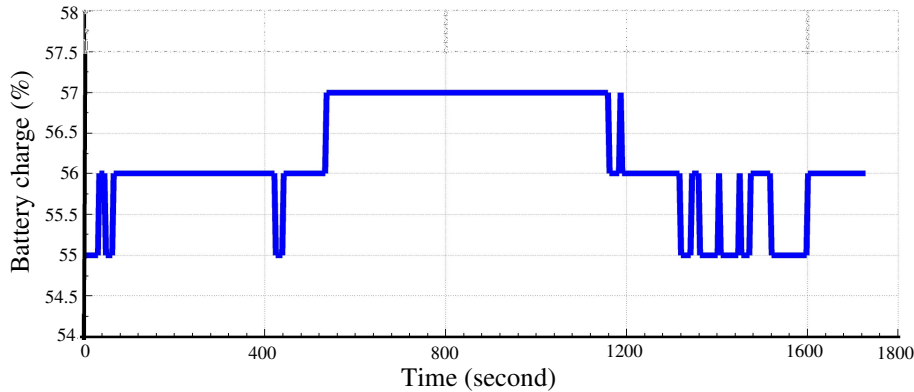


Fig. 9 Battery charge vs. time (20°C)

4.5. Time constant of the instrument

It is observed that the measured reading stabilizes within 40 seconds. As shown in Fig. 10, the time constant noted is 40 seconds. The sensing probe has been dipped in the fully charged and fully discharged solutions. The instrument takes 40 seconds to reach the maximum level. Theoretically calculated time constant, i.e., 8 seconds, is less than the observed time constant of the instrument because the system takes more time to make averaging of samples. Time constant = (maximum reading – minimum reading) \times 63.2% = (1.26 – 1.1) \times 63.2% = 8 second.

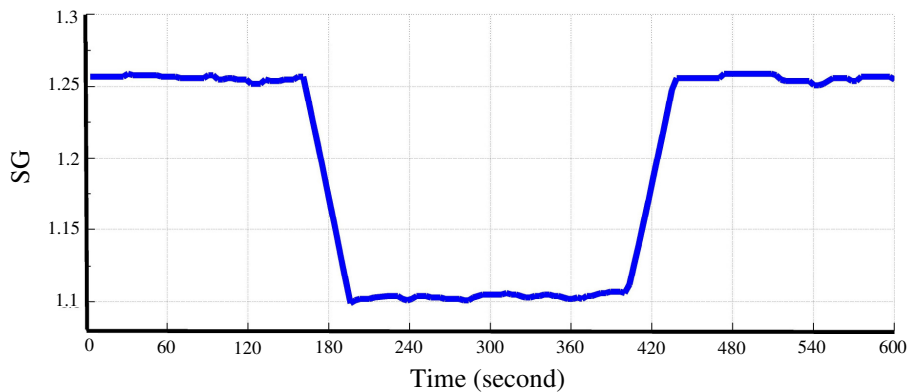


Fig. 10 Time response of MEMS hydrometer for SG measurement

4.6. Comparison of the standard hydrometer method and the proposed method

The air purge tube has been dipped in 5 different samples of SG. The SG of every sample is measured using a mechanical-type glass hydrometer as a standard method. By using the proposed MEMS hydrometer, the response of the SG and the SoC of the battery (%) is noted, as summarized in Table 4.

The graph between the standard hydrometer and the proposed MEMS hydrometer is almost accurate and linear as shown in Fig. 11. SG error between the standard and the proposed method (MPXV4006 DP) is $\pm 0.002 = 99.998\%$, and SG error between the standard method and hydrometer integrated ultrasonic (HC-SR04) sensor [22] is $\pm 0.01 = 99.99\%$. Hence, the standard glass hydrometer accuracy is $\pm 0.005 = 99.995\%$.

Table 4 Validation of proposed experimental method and glass hydrometer with Proteus

No.	Glass hydrometer	Amplified sensor output (V)	Battery charge (%)	SG	SG (Proteus simulation)	Battery (%) (Proteus simulation)
1	1.10	0.014	02	1.104	1.099	0
2	1.14	1.223	24	1.138	1.137	24
3	1.18	2.317	48	1.185	1.172	46
4	1.22	3.500	74	1.230	1.210	69
5	1.26	5.000	98	1.259	1.258	99

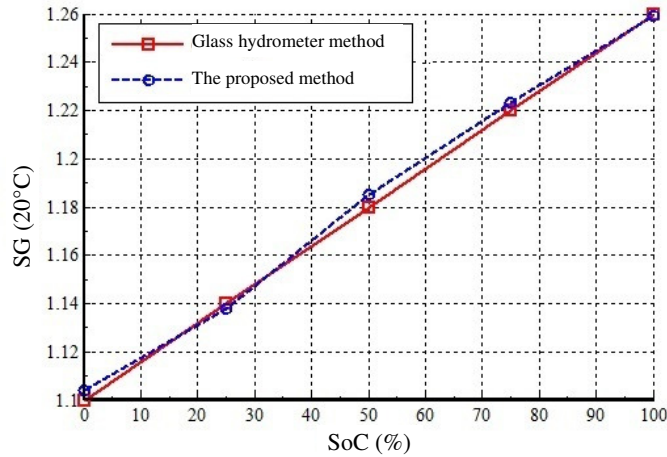


Fig. 11 Comparison of the proposed method using glass hydrometer

4.7. Linearity and sensitivity testing and comparison with optical fiber sensor

An optical fiber sensor [13] has an output of a minimum of 1 V and a maximum of 4 V for a change in the SG from 1.1 to 1.26, respectively. A refractometric optical sensor has an output of a minimum of 0.25 V and a maximum of 2.5 V for a change in the SG from 1.1 to 1.26, respectively [15]. The sensitivity of the MPXV4006DP MEMS sensor increases if the range of the amplified signal is increased more than that of the optical sensor. Hence, to increase sensitivity, MPXV4006DP MEMS sensor output is amplified from 0 V to 5 V for the same range of SG using R_g .

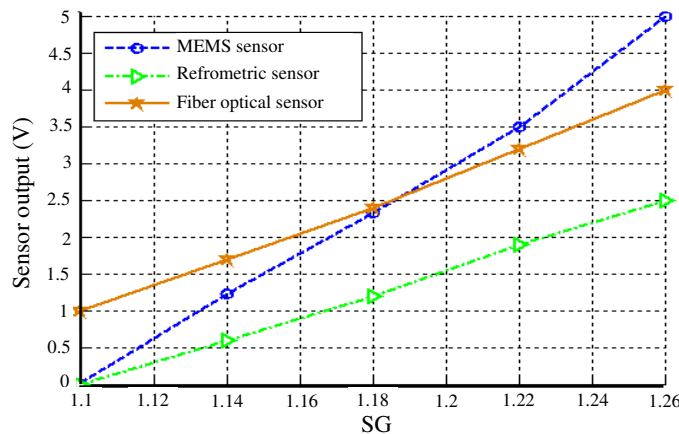


Fig. 12 Comparison of MEMS, refrometric, and fiber optical sensors

The sensitivity of the sensor can be calculated using the formula, sensitivity = the change in output/change in input. The sensitivity of the optical fiber sensor is 18, the refractometric optical sensor has a sensitivity of 14, and the sensitivity of the MEMS sensor is 32. The sensitivity of the MPXV4006DP MEMS sensor is significantly higher than that of the optical fiber sensor and the refractometric optical sensor, as the MEMS sensor has a larger slope than optical sensors. Four samples have been examined to get the variation of the sensor output concerning SG. As shown in Fig. 12, it is observed that the amplified output of the MPXV4006DP MEMS sensor is directly proportional to the SG of the lead-acid battery.

4.8. Effect of temperature on change of the SG of electrolyte solution

As shown in Fig. 13, the temperature effect on SG variation is simulated at 10°C and 40°C using Proteus. The solution of electrolyte exposed to different temperature conditions using a borosilicate glass pot, heater, and reading of the system has been analyzed to observe the effect of varying temperatures. When the temperature of the electrolyte is high at 40°C, the SG decreases, and when the temperature becomes low, i.e., 10°C, SG increases, and observations are noted in Table 5. As shown in Fig. 14, the temperature effect on SG variation is observed at 10°C and 40°C. As shown in Fig. 13, with changes in temperatures, SG varies slightly but keeps linearity constant.

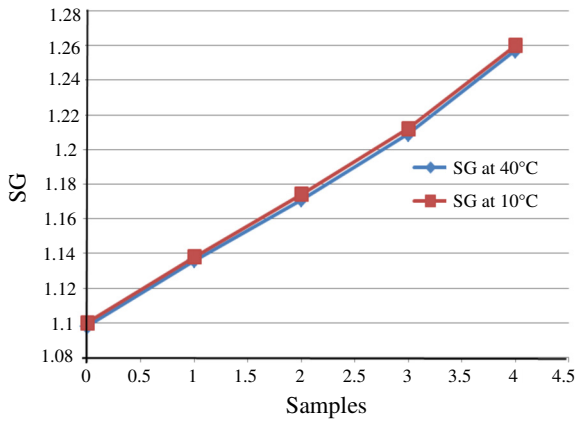


Fig. 13 SG measurement with Proteus at different temperatures

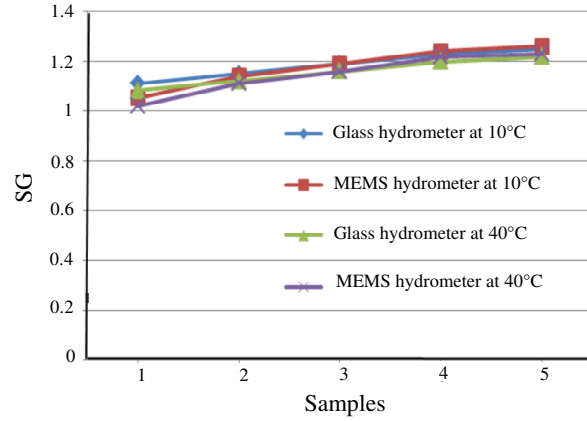


Fig. 14 SG measurement with glass and MEMS hydrometer at different temperatures

Table 5 Variation in the SG measured using glass and MEMS hydrometer at 10°C and 40°C

No.	Temperature 10°C			Temperature 40°C		
	Glass hydrometer	SG	SG (Simulation)	Glass hydrometer	SG	SG (Simulation)
1	1.11	1.05	1.10	1.08	1.02	1.098
2	1.15	1.14	1.138	1.12	1.11	1.136
3	1.19	1.19	1.174	1.16	1.16	1.171
4	1.23	1.24	1.212	1.20	1.22	1.209
5	1.25	1.26	1.260	1.22	1.23	1.257

5. Conclusions

In this study, a short air purge system integrated with the MEMS pressure sensor designed for measuring SG online has been proposed and realized. The proposed method is basic, but it can measure an extremely small change in SG with great accuracy compared to conventional methods. No extra signal conditioning is necessary for temperature compensation as it is incorporated in the software. Such an air purge system has better sensitivity and range as compared to other optical sensors. The SG with ±0.002% resolution as well as the battery charge percentage with ±1% resolution have been recorded by this MEMS-based hydrometer. In the future, auto-calibration of the measurement system can be considered, as it can be useful in fixing errors. This technique can also be utilized to measure the SG of milk, seawater, ethylene glycol, benzene, refrigerant R-22, and crude oil in process industries.

Acknowledgment

The authors sincerely thank the Instrumentation and Control Department, College of Engineering, Pune (COEP) for the financial support in filing a patent and publication.

Abbreviations and Symbols

SoC	State-of-charge	SG	Specific gravity
LM35	Linear monolithic	MEMS	Micro electro mechanical system
ΔP	Differential pressure	v_1	Output voltage of the MPXV4006DP sensor
H	Head between the tubes	v_2	Zero adjustment voltage
Δp	Change in the density of acid	v_0	Amplified output voltage of AD-620
g	Gravitational constant	G	Gain of AD-620
x_{temp}	SG of the environmental factor	$x_{20^\circ C}$	SG of the solution at 20°C
$temp$	Acid temperature of the lead-acid battery	DR	Discharge rate
R_g	Gain resistor		

Conflicts of Interest

The authors declare no conflict of interest.

References

- [1] S. Kim, M. Kwon, and S. Choi, "Operation and Control Strategy of a New Hybrid ESS-UPS System," IEEE Transactions on Power Electronics, vol. 33, no. 6, pp. 4746-4755, June 2018.
- [2] M. Lei, Z. Yang, Y. Wang, H. Xu, L. Meng, J. C. Vasquez, et al., "An MPC-Based ESS Control Method for PV Power Smoothing Applications," IEEE Transactions on Power Electronics, vol. 33, no. 3, pp. 2136-2144, March 2018.
- [3] A. Clerici, E. Tironi, and F. C. Dezza, "Multiport Converters and ESS on 3-kV DC Railway Lines: Case Study for Braking Energy Savings," IEEE Transactions on Industry Applications, vol. 54, no. 3, pp. 2740-2750, May-June 2018.
- [4] B. Vulturescu, S. Butterbach, and C. Forgez, "Experimental Considerations on the Battery Lifetime of a Hybrid Power Source Made of Ultracapacitors and Lead-Acid Batteries," IEEE Journal of Emerging and Selected Topics in Power Electronics, vol. 2, no. 3, pp. 701-709, September 2014.
- [5] M. Greenleaf, O. Dalchand, H. Li, and J. P. Zheng, "A Temperature-Dependent Study of Sealed Lead-Acid Batteries Using Physical Equivalent Circuit Modeling with Impedance Spectra Derived High Current/Power Correction," IEEE Transactions on Sustainable Energy, vol. 6, no. 2, pp. 380-387, April 2015.
- [6] P. B. L. Neto, O. R. Saavedra, and L. A. de S. Ribeiro, "A Dual-Battery Storage Bank Configuration for Isolated Microgrids Based on Renewable Sources," IEEE Transactions on Sustainable Energy, vol. 9, no. 4, pp. 1618-1626, October 2018.
- [7] J. M. Acevedo, A. M. C. Paz, S. Fernandez-Gomez, and M. L. Soria, "Life Testing of Plastic Optical Fibers for Lead-Acid Battery Fast Charge Equipment," Annual Reliability and Maintainability Symposium, pp. 126-131, January 2008.
- [8] A. M. C. Y. Paz, J. M. Acevedo, J. D. Gandoy, and A. del R. Vazquez, "Multisensor Fibre Optic for Electrolyte Density Measurement in Lead-Acid Batteries," IECON 2006 - 32nd Annual Conference on IEEE Industrial Electronics, pp. 3012-3017, November 2006.
- [9] C. Y. Patil and Y. G. Adhav, A Lead Acid Battery Charge Monitoring System, Indian Patent, 15/2020,16896, April 10, 2020.
- [10] J. Mucko, "A Possibility of the State of Charge Monitoring of the Lead-Acid Battery by Means of Current Pulses of a Given Value," 14th Selected Issues of Electrical Engineering and Electronics (WZEE), article no. 8748988, November 2018.
- [11] S. Piller, M. Perrin, and A. Jossen, "Methods for State-of-Charge Determination and Their Applications," Journal of Power Sources, vol. 96, no. 1, pp. 113-120, June 2001.
- [12] P. Křivk, "Methods of SoC Determination of Lead Acid Battery," Journal of Energy Storage, vol. 15, pp. 191-195, February 2018.
- [13] G. P. Hancke, "A Fiber-Optic Density Sensor for Monitoring the State-of-Charge of a Lead Acid Battery," IEEE Transactions on Instrumentation and Measurement, vol. 39, no. 1, pp. 247-250, February 1990.
- [14] M. Zhao, J. Long, Y. Chen, B. B. Luo, and J. Liu, "Surplus Electric Quantity Online Examination System of Lead-Acid Battery Based on ARM," World Automation Congress, pp.1-4, September 2008.

- [15] S. S. Patil, V. P. Labade, N. M. Kulkarni, and A. D. Shaligram, "Analysis of Refractometric Fiber Optic State-of-Charge (SoC) Monitoring Sensor for Lead Acid Battery," *Optik*, vol. 124, no. 22, pp. 5687-5691, November 2013.
- [16] A. Hossain and M. J. Dwyer, "A New Type of Liquid Density Transducer Based on the Principle of Linear Variable Differential Transformer," *SIcon/01. Proceedings of the First ISA/IEEE. Sensors for Industry Conference (Cat. No.01EX459)*, pp. 270-275, November 2001.
- [17] M. Morbel, H. J. Kohnke, and J. Helmke, "Monitoring of Lead Acid Batteries Continuous Measurement of the Acid Concentration," *INTELEC 05 - Twenty-Seventh International Telecommunications Conference*, pp. 263-268, September 2005.
- [18] A. M. Cao-Paz, L. Rodríguez-Pardo, and J. Fariña, "Density and Viscosity Measurements in Lead Acid Batteries by QCM Sensor," *IEEE International Symposium on Industrial Electronics*, pp.1290-1294, June 2011.
- [19] X. Lu, L. Hou, L. Zhang, Y. Tong, G. Zhao, and Z. Y. Cheng, "Piezoelectric-Excited Membrane for Liquids Viscosity and Mass Density Measurement," *Sensors and Actuators A: Physical*, vol. 261, pp. 196-201, July 2017.
- [20] M. Heinisch, T. Voglhuber-Brunnmaier, E. K. Reichel, I. Dufour, and B. Jakoby, "Application of Resonant Steel Tuning Forks with Circular and Rectangular Cross Sections for Precise Mass Density and Viscosity Measurements," *Sensors and Actuators A: Physical*, vol. 226, pp. 163-174, May 2015.
- [21] T. L. Wilson, G. A. Campbell, and R. Mutharasan, "Viscosity and Density Values from Excitation Level Response of Piezoelectric-Excited Cantilever Sensors," *Sensors and Actuators A: Physical*, vol. 138, no. 1, pp. 44-51, July 2007.
- [22] C. Tang and J. T. Lin, "Online Autonomous Specific Gravity Measurement Strategy for Lead-Acid Batteries," *IEEE Sensors Journal*, vol. 20, no. 4, pp. 1980-1987, February 2020.
- [23] K. W. Park and H. C. Kim, "High Accuracy Pressure Type Liquid Level Measurement System Capable of Measuring Density," *TENCON 2015 - 2015 IEEE Region 10 Conference*, article no. 7372925, November 2015.
- [24] J. Y. Kim, S. E. Bae, T. H. Park, S. W. Paek, T. J. Kim, and S. J. Lee, "Wireless Simultaneous Measurement System for Liquid Level and Density Using Dynamic Bubbler Technique: Application to KNO_3 Molten Salts," *Journal of Industrial and Engineering Chemistry*, vol. 82, pp. 57-62, February 2020.
- [25] C. Zhang, Y. Huang, Y. Fang, P. Liao, Y. Wu, H. Chen, et al., "The Liquid Level Detection System Based on Pressure Sensor," *Journal of Nanoscience and Nanotechnology*, vol. 19, no. 4, pp. 2049-2053, April 2019.
- [26] Y. Guo, "A Sensor of Sulfuric Acid Specific Gravity for Lead-Acid Batteries," *Sensors and Actuators B: Chemical*, vol. 105, no. 2, pp. 194-198, March 2005.
- [27] C. Liu, W. Ren, B. Zhang, and C. Lv, "The Application of Soil Temperature Measurement by LM35 Temperature Sensors," *Proceedings of 2011 International Conference on Electronic & Mechanical Engineering and Information Technology*, vol. 4, pp. 1825-1828, August 2011.



Copyright© by the authors. Licensee TAETI, Taiwan. This article is an open access article distributed under the terms and conditions of the Creative Commons Attribution (CC BY-NC) license (<https://creativecommons.org/licenses/by-nc/4.0/>).